Malaysian Journal of Catalysis
http://mjcat.utm.my/
MJCat
Research Article

Direct Alcoholysis of Glucose into Alkyl Levulinates Catalysed by Metal-Doped Sulfonated Activated Carbon

Kirrthana Krishnasamy[1], Chee Shu Yi[1], Mohd Asmadi[1*], Zaki Yamani Zakaria[1], Muzakkir Mohammad Zainol[2], Sureena Abdullah[3]

[1] *Faculty of Chemical and Energy Engineering, Universiti Teknologi Malaysia, 81310 Johor Bahru, Johor, Malaysia*
[2] *School of Chemical Engineering, College of Engineering, Universiti Teknologi Mara, 40450, Shah Alam, Selangor, Malaysia*
[3]*Faculty of Chemical and Natural Resources Engineering, Universiti Malaysia Pahang, 26300, Gambang, Pahang, Malaysia*

**Corresponding Author: mohdasmadi@utm.my*

Article history:
Received 01 September 2024
Accepted 30 October 2024

ABSTRACT

Lignocellulosic biomass is widely studied to produce alkyl levulinate through acid catalyst catalysed alcoholysis, which potentially used as a biofuel additive. However, the poor properties of homogeneous catalyst have prompted this study to focus on enhancing the yield of alkyl levulinate by using sulfonated activated carbon (AC-S) doped with different metals as a heterogeneous catalyst with co-existence of Brønsted and Lewis acidic sites. The activated carbon (AC) precursor was modified via sulfonation and impregnated with iron (Fe), copper (Cu) and cobalt (Co) metals, which were further characterised to evaluate their physicochemical properties as a catalyst. Their catalytic activity was then evaluated for glucose alcoholysis in a stainless-steel batch reactor at 180 ˚C for 4 h, by charging 0.6 g of glucose, 40 mL of alcohol (methanol and ethanol) and 0.3 g of catalyst. According to the results, the catalysts' catalytic activity was improved after sulfonation and metal doping. Among the employed heterogeneous catalysts, AC-S-Cu exhibited the highest catalytic activity, which was contributed mainly by its co-existence of Brønsted and Lewis acidic sites with significant Brønsted acidity, higher thermal stability with minimum weight loss up to 200 ˚C (<2 wt%), better morphology, and larger surface area (928 m^2/g) compared to other metal-doped AC-S. The maximum alkyl levulinate yield (15.04 wt%) was obtained for ethyl levulinate production under conditions of 180 ˚C, 4 hr, 0.6 g of glucose, 0.3 g of AC-S-Cu and 40mL of ethanol. The outcome of this study provides an insight on the potential of AC-S-Cu in facilitating the direct alcoholysis of glucose to alkyl levulinate.

Keywords: *alkyl levulinate; Brønsted-lewis; alcoholysis; sulfonated activated carbon; metal doping*

| eISSN 0128-2581 |

1. INTRODUCTION

Climate change, energy security, and heavy dependence on fossil fuels are among global issues that require immediate attention. Biofuels have emerged as a sustainable alternative energy source via the use of biomass as a promising feedstock. Biomass mainly consists of cellulose, hemicellulose and lignin, often being utilized in the conversion of high value products such as levulinic acid (LA) and alkyl levulinate (AL) [1]. AL is a promising renewable fuel additive used to improve engine performance and produce greener emissions.

Due to the high chemical cost and complex synthesis route involving multiple steps from the easily accessible levulinic acid (LA) and furfuryl alcohol (FA) through esterification, the single-step approach of direct conversion of lignocellulose-derived sugars into AL has attracted interest [2]. As a result, monosaccharides like glucose is commonly used as a representative material for biomass conversion studies as it is easier to be converted compared to polysaccharides and biomass which have stronger and more complex hydrogen bonds and Van Der Waals forces [3].

The direct AL production involves the esterification of monosaccharides with alcohol by employing acidic catalysts to promote the AL yields. Despite the cost-effectiveness and efficiency of the commonly used homogeneous catalyst such as sulfuric acid and hydrochloric acid, these acids present significant drawbacks related to environmental concerns such as lower recyclability and corrosion issues [4]. As an alternative, heterogeneous catalyst was introduced to tackle these issues. Various heterogenous catalysts such as metal sulphates, sulphated metal chlorides, heteropolyacids, zeolites and resins have been previously employed in monosaccharides conversion to AL. However, those heterogenous catalysts have drawbacks such as poor surface properties and fast catalyst deactivation [4]. As researches lately work towards

establishing green conversions, activated carbon (AC) is an emerging carbon-based heterogeneous catalyst. Activated carbons are well-known for their large surface area and adjustable surface functional groups providing specific properties, encouraged many researchers to employ it in the conversions of biomass to AL [5,6].

Many research projects have aimed to produce AL via heterogeneous acid catalyst with the combination approach of Brønsted-Lewis acids as they found that the combined effect of both acids have enhanced the reaction process by the following the pathway shown in Figure 1 [7]. The Brønsted-Lewis dual-acidity facilitates the glucose conversion to AL in such a pathway that requires lesser energy and hence enhances the AL yields [8]. This is in agreement with Tempelman et al. 2023 [5] which proved that the dual acidic tin-doped sulfonated activated carbon (Sn-Fn-AC) showed high activity towards the production of 5-HMF from glucose-fructose-sucrose aqueous solution as compared to the mono-acidic catalyst, where 30 mol% 5-HMF yield was obtained using Sn-Fn-Ac, while less than 5 mol% 5-HMF yield was reported using mono-acidic Fn-AC..

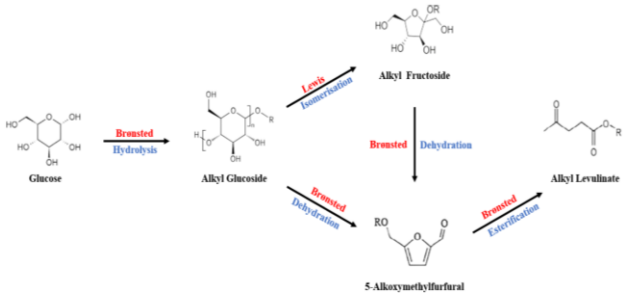

Figure 1. Roles of Brønsted and Lewis acid in facilitating AL conversions

Although several studies have employed AC-S in the biomass conversion to AL, research works on the employment of dual-acidity AC-S as a catalyst in direct glucose conversion to AL is scarcely reported. To the best of our knowledge, the synthesis of dual-acidity AC-S catalyst by metal doping with copper, cobalt and iron sulfates; and employing them in the direct glucose conversion AL have not been reported in literatures. Accordingly, this study aims to evaluate AL yield from direct glucose conversion through alcoholysis reaction catalyzed by newly developed catalysts. Sulfonation and metal doping were performed on the AC precursor to provide the joined acidities of Brønsted-Lewis. The catalysts were then characterized and employed in the conversion of glucose to two different ALs, namely methyl levulinate (ML) and ethyl levulinate (EL).

2. METHODOLOGY

All materials were purchased from Sigma Aldrich, VChem and Merck, ensured are analytical grade and were used as received. Commercialized activated carbon, concentrated sulfuric acid (H_2SO_4, 95-97 %), iron (II) sulfate heptahydrate ($FeSO_4{\cdot}7H_2O$), copper sulfate pentahydrate ($CuSO_4{\cdot}5H_2O$), cobalt sulfate heptahydrate ($CoSO_4{\cdot}7H_2O$) were used for the synthetization of heterogeneous catalyst. Meanwhile, pyridine was used for the catalyst characterization. The conversion of glucose to AL was conducted using methanol (CH_3OH), ethanol (C_2H_5OH, 95%), and glucose ($C_6H_{12}O_6$).

2.1 Catalyst Preparation

In this study, five different AC catalysts were prepared. In order to prepare AC-S, 10.0 g of AC was mixed with 100 mL of H_2SO_4 in 150 mL round bottom flask equipped with a magnetic stir bar and condenser. The mixture was then stirred at 300 rpm with heating at 373 K for 5 h. After the treatment, the mixture was diluted by adding 2 L of distilled water prior to vacuum filtration in a Büchner flask until the cleaning water pH was approximately 7. The sample was placed in a crucible and oven dried at 110 ˚C for 24 h. The dried sample was labelled as AC-S.

Next, the AC-S was further mixed with 10 g of $FeSO_4.7H_2O$ which was pre-dissolved in 100ml distilled water in a 1 L beaker under 500 rpm stirring at room temperature for 2 h. The mixture was then filtered under suction and dried in the oven for 110 ˚C overnight before further calcined for 5 h at 300 ˚C. The dried sample was designated as AC-S-Fe. The same procedure was used to prepare AC-S-Cu and AC-S-Co using $CuSO_4{\cdot}5H_2O$ and $CoSO_4{\cdot}7H_2O$ respectively.

2.2 Catalyst Characterization

The thermal stability and degradation of the prepared catalysts were determined by Thermogravimetric Analysis (TGA) using TGA Q500 V20.13 Build 39 through inert heating from 30 to 950 ˚C with a heating rate of 10 ˚C/min. The presence of functional groups of catalyst was confirmed by Fourier transform infrared (FTIR) spectroscopy from Perkin Elmer Spectrum using KBr pellets in the IR range of 370 - 4000 cm^{-1}. Next, the catalyst's phase structure and crystallinity were studied via X-ray diffraction (XRD) analysis, which ranges from 3 ° to 100 ° 2θ with a step size of 0.02 ° and step time of 60 s, operated at 40 kV and 30 mA with a fixed 2/3° incident slit on the X-ray diffractometer (D/teX Ultra 250 Rigaku SmartLab with an attachment of ASC robot- reflection) via Cu Kα radiation.

The elemental analysis and morphology of the samples were carried out using energy-dispersive X-ray (EDX) spectrometry coupled with Scanning Electron Microscopy (SEM) (Hitachi SU3500). The surface area and pore distribution were measured using Micromeritics 3-Flex instrument. The samples were degassed under vacuum at 200 ˚C for 6 h before conducting standard nitrogen (N_2) adsorption and desorption at -196 ˚C. The Brunauer-Emmett Teller (BET) method was used to calculate the total surface area, whereas Barrett-Joyner-Halenda (BJH) and t-plot methods were utilized to differentiate between the

micropores and mesopores volume associated with the surface area.

The acidity of the catalysts were determined by Ammonia-Temperature Program Desorption (NH_3-TPD) analysis. The analysis was conducted using Chemisorption Analyzer Micromeritics Autochem II, and degassing temperature was set at 150 °C. For the determination of acidity type for Brønsted-Lewis acid, the characterization was carried out using FTIR with pyridine as a probe. 50 mg of sample was dried at 115 ˚C for 1 h and cooled to room temperature, then 0.5 mL of pyridine was directly added into the sample in a glass vial and left for 1 h for a complete adsorption. The pyridine added sample was dried at 120 ˚C for 1 h then the sample was allowed to cool until room temperature. The dried sample was analyzed in the spectral region between 1400 and 1700 cm^{-1} using alkali halide (KBr) pellets. The ratio of Brønsted to Lewis acid sites can be computed using Equation (1).

$$\text{Ratio of Brønsted to Lewis Acidity} = \frac{A_B \times C_L}{A_L \times C_B} \quad (1)$$

Where, A_B and A_L are the areas of Brønsted and Lewis acidity from FTIR (cm^{-1}), respectively, C_B and C_L is the coefficient of Brønsted and Lewis acidity (188 cm/mmol) and (142 cm/mmol).

2.3 Direct Alcoholysis of Glucose to AL

The alcoholysis of glucose was carried out in a 150 mL stainless steel batch reactor. The reactor was charged with 0.6 g of glucose, 0.3 g of AC and 40 mL of ethanol. The solution was then heated to 180 °C and stirred at 200 rpm for 4 h. Once the reaction was completed, the reactor was cooled to room temperature. The resulting reaction mixture was then filtered through a syringe filter (PTFE, 0.45 µm, VWR) prior to Gas Chromatograph-Flame Ionization Detector (GC-FID) analysis. Similar steps were taken for all AC-S, AC-S-Fe, AC-S-Cu and AC-S-Co to determine its catalytic activity. The experiment was repeated using methanol as solvent.

2.4 Product Analysis

To calculate the AL yields in the sample product, the resulting liquid undergoes analysis using GC-FID. The AL peak areas were identified using an Agilent Technology 7820A GC-FID system equipped with a DB-Wax column (30 m × 0.25 mm × 0.25 µm). The analysis conditions used were as follows: N_2 as the carrier gas with 1.0 mL/min of flow rate, the injection port temperature of 250 ˚C, the detector temperature of 270 ˚C, and the oven temperature programmed from 50 to 170 ˚C (5 ˚C/min), followed by 170-240 ˚C (15 ˚C/min). Standard calibration curve of AL standard solution was constructed to derive the equation for ALs concentration calculation in the product sample. The ALs yields were calculated using Equation (2).

$$\text{ALs Yield (wt \%)} = \frac{Concentration\ of\ ALs\left(\frac{g}{mL}\right) \times Volume\ of\ product\ (mL)}{Amount\ of\ Initial\ Glucose\ (g)} \text{ x } 100\% \quad (2)$$

3. RESULTS AND DISCUSSION

3.1 Catalyst Characterization

The TGA/DTG curve is shown in Figure 2a. Activated carbon exhibits lowest thermal stability due to its lower activation energy for oxidation of amorphous structure [1], whereby its thermal stability increases after sulfonation as AC is affected by strong acid on the carbon structure. Further modification of AC-S with metal doping increases the thermal stability of the sample, which was contributed by the high thermal stability of metals itself [7]. It is observed that 2.5 wt% weight loss in the 270–330 °C temperature region, which could be attributed to decomposition of the $–SO_3H$ groups [5]. Since the alcoholysis reaction was carried out at 180°C, all the metal doped sulfonated activated carbon showed good thermal stability up to 400 °C and are suitable to be employed in the conversion process as there is no drastic weight loss indicated in TGA curves below 180 °C.

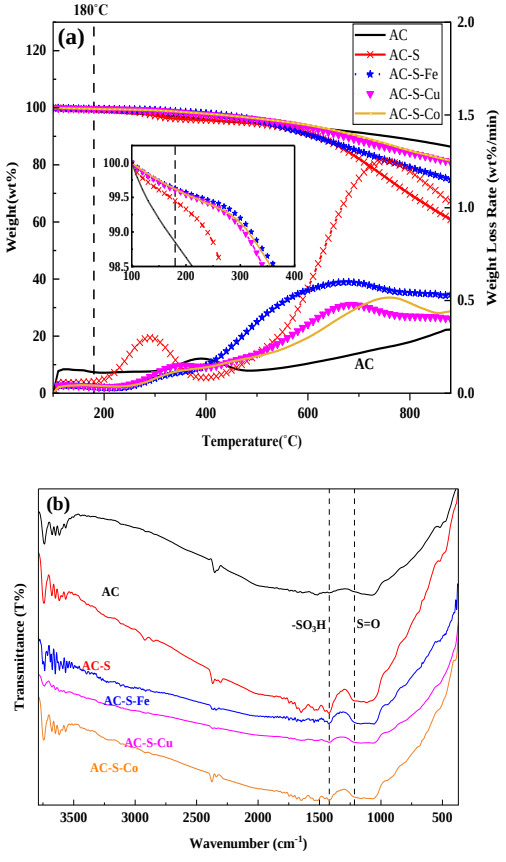

Figure 2. (a) TGA-DTG thermographs and (b) FTIR spectra of AC, AC-S, AC-S-Fe, AC-S-Cu and AC-S-Co

Figure 2b represents the FTIR spectra of the catalysts. A distinct vibration is evident between 3800 cm^{-1} and 3500 cm^{-1}, indicating O-H stretching and the generation of hydroxyl groups, along with adsorbed water on the surface of the carbon [9]. The existence of S=O stretching and $-SO_3H$ bonding in the range of 1350 cm^{-1} and 1020 cm^{-1} corresponds to the introduction of SO_3H groups, which signifies the effective attachment of $-SO_3H$ groups onto the activated carbon surface in all the catalysts except AC. For samples doped with metal, a noticeable peak appears within the range of 570 cm^{-1} to 400 cm^{-1}. Two additional small peaks at 384 cm^{-1} and 400 cm^{-1} were identified indicating the presence of Fe-O and Co-O bonds respectively following the impregnation process [2,10].

The crystallinity of prepared catalysts was observed using XRD analysis and the spectrum derived is depicted in Figure 3a. All the synthesized carbon materials display two well-defined diffraction peaks at 2θ angles around 23° and 42°, with varying intensities, which indicated a disordered activated carbon sheet structure. There are minor crystal peaks in the range of 30° to 40° associated with iron oxide (FeO). This is attributed to the interaction between the Fe species and the AC-S structure, resulting in reduced crystallinity of the amorphous peak which agrees with the literature data [7].

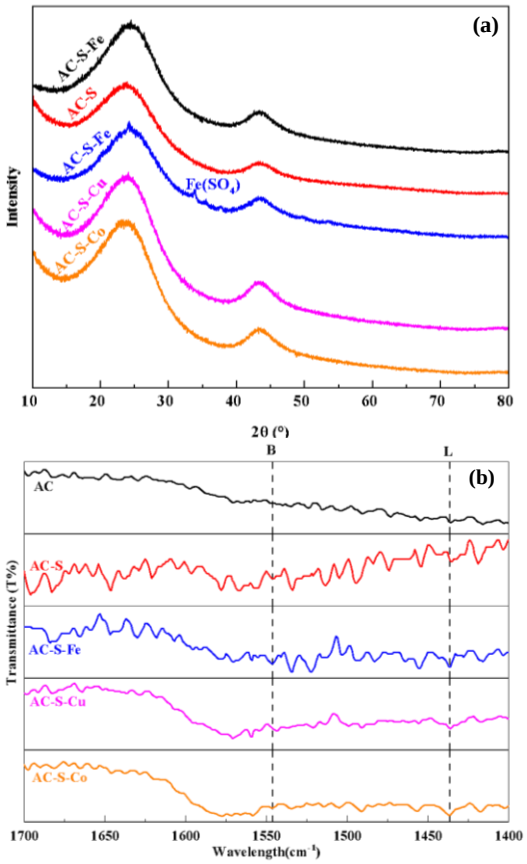

Figure 3. (a) XRD and (b) Pyridine-FTIR spectra of AC, AC-S, AC-S-Fe, AC-S-Cu and AC-S-Co (B: Brønsted, L: Lewis)

However, the small peak of metal elements was not clearly observed by both FTIR and XRD spectrums, which could be due to the presence of low Fe, Cu and Co species on the AC-S structure. The existence of $-SO_3H$ and metal elements on the surface of the activated carbon was confirmed through EDX analysis, as tabulated in Table 1. The presence of sulfur (S) in the AC-S sample confirmed the successful sulfonation of the activated carbon. The trace amount of sulfur in the AC sample may be attributed to contamination during sample preparation. Additionally, the detection of Fe, Cu, and Co elements in the AC-S-Fe, AC-S-Cu, and AC-S-Co samples respectively indicates the effective and uniform doping of each metal onto the activated carbon surface.

Table 1: Composition of element contained in AC, AC-S, AC-S-Fe, AC-S-Cu and AC-S-Co

Catalyst	Element Weight (%)						
	C	O	S	Fe	Cu	Co	N
AC	87.0	12.1	0.8	-	-	-	0.1
AC-S	87.7	10.1	2.2	-	-	-	
AC-S-Fe	68.6	11.7	2.0	17.7	-	-	0.1
AC-S-Cu	83.9	6.2	1.4	-	8.2	-	0.3
AC-S-Co	86.4	8.1	1.3	-	-	3.9	0.3

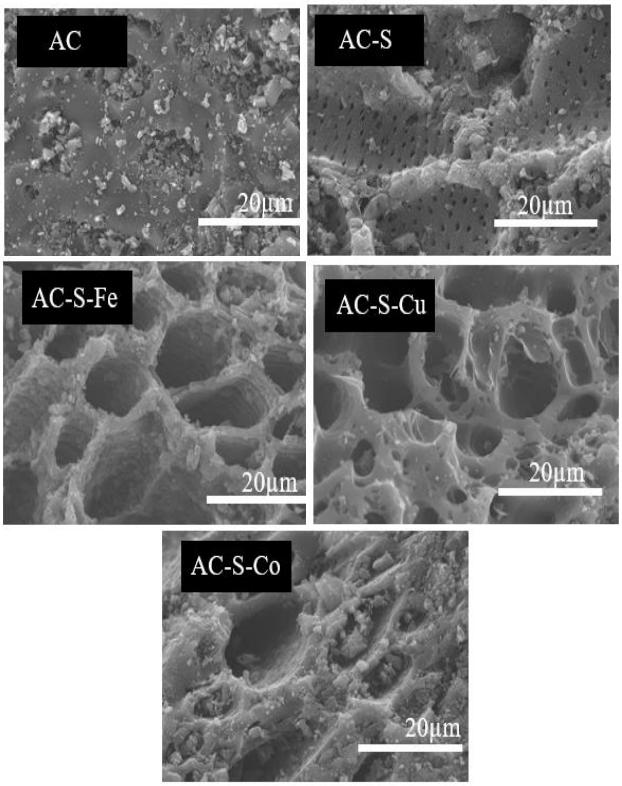

Figure 4. SEM images of AC, AC-S, AC-S-Fe, AC-S-Cu and AC-S-Co

Figure 3b shows the pyridine-FTIR spectra of the prepared catalysts. An absorption peak near 1450 cm^{-1} indicates the presence of Lewis acidic sites, whereas an absorption peak near 1540 cm^{-1} represents Brønsted acidic sites [14,15]. The Brønsted to Lewis ratios of AC, AC-S, AC-S-Fe, AC-S-Cu and AC-S-Co were calculated to be 0.48, 1.51, 0.73, 0.81 and 0.66. The introduction of sulfonic acid increases the B/L ratio due to the contribution of Brønsted acid sites increases. The B/L ratio decreases after metal doping attributed to the significant presence of strong Lewis acidic metals.

The surface morphology of prepared catalysts is presented by SEM images in Figure 4. The irregular particles with a rough surface are observed for all samples suggested that activated carbon exhibited numerous micropores on the surface, ultimately contributing to an increased material surface area. The high acid treatment during sulfonation process leads to some development of tiny pores, which exposes a larger surface area for reactions. In addition, the metal doped ACs showed better morphology than AC due to the more open structure for the reaction with the formation of acid sites.

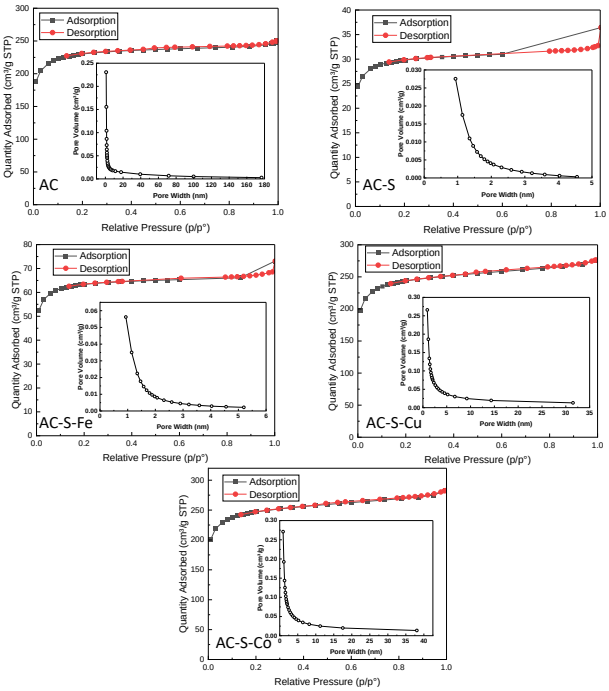

Figure 5. N_2 adsorption-desorption isotherms and BJH pore size distributions of AC, AC-S, AC-S-Fe, AC-S-Cu and AC-S-Co

Surface area and porosity of the catalyst are other major factors influencing catalytic activity in providing high EL yield. Figure 5 displays the N_2 adsorption-desorption isotherms and pore size distribution. The isotherms obtained for the synthesized catalysts fit the II-type adsorption and correspond to an H4-type hysteresis loop based on the IUPAC classification as expected from literature data [11]. This indicates the formation of microporous structures and the existence of aggregates of plate-like particles, leading to the creation of slit-shaped pores with irregular sizes and shapes. Table 2 and 3 summarizes the surface area and porosity of the catalysts. The parent material (AC) contains a BET surface area of 881 m^2/g, which decreases to 114 m^2/g after sulfonation and increases again after introduction of metals. This decrease indicates SO_3H groups were added not only to the surface of the AC material but also occupied some of the pore openings, as proved by the previous findings [4,12]. A subsequent increment in S_{BET} and V_{pore} was observed after metal doping. The addition of metals in the forms of nanoparticles after metal-doping prevents the agglomeration of carbon particles, resulting in a more dispersed structure by having increased volume of micropores, and thus the surface area increases [6,13]. Catalyst with higher surface area is always preferred for catalytic reactions as they have more available active sites for the reaction to take place, and thus more reaction can occur simultaneously leading to higher product yields. This trend was aligned with the SEM result, where the metal-doped AC-S was more porous, which exposed more active sites and favors the reaction.

Table 2: Surface area and porosity of AC, AC-S, AC-S-Fe, AC-S-Cu and AC-S-Co

Catalyst	Surface Area (m^2/g)		
	S_{BET}[a]	S_{Meso}[b]	S_{Micro}[c]
AC	881	213	667
AC-S	114	27	87
AC-S-Fe	243	52	191
AC-S-Cu	929	237	691
AC-S-Co	939	248	692

[a] BET surface area was obtained from the N_2 adsorption isotherm.
[b] Surface areas of mesopore were obtained from the t-plot method.
[c] Surface areas and pore volume of micropore were obtained from the t-plot method.

Table 3: Porosity of AC, AC-S, AC-S-Fe, AC-S-Cu and AC-S-Co

Catalyst	Pore volume (cm^3/g)			Pore diameter (nm)
	V_{Pores}[a]	V_{Meso}[b]	V_{Micro}[c]	D_{Mean}[d]
AC	0.39	0.12	0.27	1.75
AC-S	0.05	0.02	0.03	1.78
AC-S-Fe	0.11	0.03	0.08	1.75
AC-S-Cu	0.43	0.15	0.28	1.84
AC-S-Co	0.44	0.16	0.28	1.86

[a] Pore volume was obtained from the single-point desorption method.
[b] Volume of mesopore = (V_{pores} - V_{micro}).
[c] Estimated from the adsorption average pore diameter (4 V/A by BET).
[d] Estimated from the BJH desorption average pore diameter (4 V/A).

The NH_3-TPD profiles of the five different catalysts is depicted in Figure 6 and their acidity values are shown in Table 4. The desorption temperature and the intensity of the peaks is associated with the catalysts' acidic number and strength. Desorption peak below 200 °C indicates the presence of weak acidic sites, 200-600 °C indicates the

presence of moderate acidic sites, while desorption peak above 600°C indicates presence of strong acidic sites. AC has the lowest acidity with low intensity peaks observed. AC-S has slightly higher acidity, with higher intensity peak at weak and moderate acidic sites regions. The sulfonation performed on AC had contributed to the increase in catalyst acidity but still weak. Interestingly, upon metal-doping the catayst's acidities greatly enhanced with AC-S-Co and AC-S-Cu reported the highest acidity of 2.81 and 2.69 mmol/g, respectively. Highest intensity peaks under all regions were observed in the NH_3-TPD profiles of the metal-doped catalysts. The metal doping had successfully enhanced the catalyst acidity contributed by the joined Brønsted and Lewis acidity, as hypothesized. According to the acidity values reported in Table 4, the order of catalyst acidity can be arranged as AC-S-Co ≈ AC-S-Cu > AC-S-Fe > AC-S > AC.

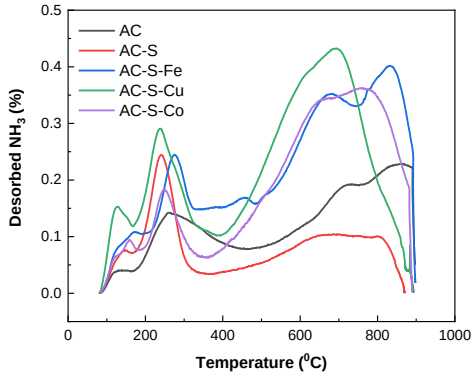

Figure 6. AC based catalysts' acidity based on NH_3-TPD profiles.

Table 4. Acidity values of AC based catalysts

Catalysts	Weak acidity (mmol/g)	Moderate acidity (mmol/g)	Strong acidity (mmol/g)	Total acidity (mmol/g)
AC	0.09	0.33	0.65	1.08
AC-S	0.42	0.58	0.62	1.62
AC-S-Fe	0.36	0.49	0.84	1.68
AC-S-Cu	0.29	1.93	0.48	2.69
AC-S-Co	0.06	0.19	2.56	2.81

3.2 Direct Alcoholysis of Glucose to AL

The AL yields obtained from glucose using these five catalysts are illustrated in Figure 7. Activated carbon acting alone as a catalyst, presented poor catalytic activity in the glucose conversion to ALs. The poor catalytic activity of AC is attributed to the absence of acidic sites in the catalyst, which is one of the main factors to facilitate ALs production from biomass carbohydrates. Fortunately, upon sulfonation the AC's catalytic activity has greatly enhanced with reported ML and EL yields of 9.87 wt% and 4.21 wt%, respectively. Brønsted acidic sites was introduced in the AC upon sulfonation, which favors the dehydration and esterification reactions that will accelerate the yielding of targeted ALs.

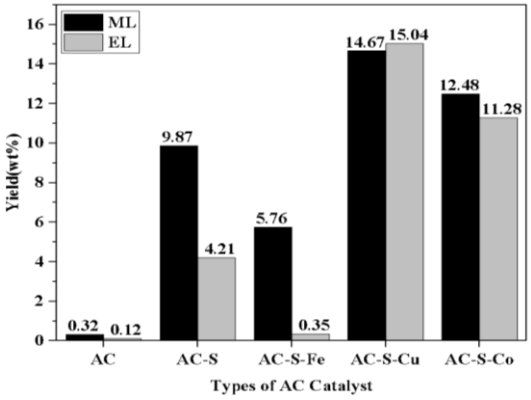

Figure 7. Alkyl levulinate yields obtained from different activated carbon catalysts (180 °C, 4 h, 0.6 g glucose, 0.3 g AC catalyst, 40 mL alcohol)

Interestingly, incorporation of metals in the AC-S had improved the AL yields for AC-S-Cu (ML: 14.67 wt%; EL: 15.04 wt%) and AC-S-Co (ML: 12.48 wt%; EL: 11.28 wt%), but reduced for AC-S-Fe (ML: 5.76 wt%; EL: 0.35 wt%). The addition of metals in the AC-S had formed catalysts with Bronsted-Lewis dual acidities, which further promoted the AL yields. AC-S-Cu exhibited the highest catalytic activity among all which was mainly due the combination of Brønsted-Lewis acidic sites with the significant Brønsted acidity, supported by the higher surface area and porosity, had increased the selectivity of AL production and further contributed to the higher AL yields [16,17]. In comparison between AL yields obtained from AC-S and AC-S-Fe, the AL yields reduced when AC-S-Fe was employed as catalyst, contradict to the hypothesis made where Brønsted-Lewis dual acidity could enhance the AL yields. As can be observed in Table 4, AC and AC-S-Fe have almost similar total acidities, however the weak and moderate acidic sites of AC are much higher compared to AC-S-Fe. Very strong acidity could shift the reaction pathway of glucose conversion to other by-products and cause high etherification of alcohol leading to solvent loss, and thus resulting in a lower yield [18]. Similar trend can be observed between AC-S-Cu and AC-S-Co, where although AC-S-Co has higher total acidity, AC-S-Cu's higher moderate acidic sites were more favourable for AL production. This elucidates that although acidic sites are required for AL production from biomass carbohydrates, it is important to properly tune the catalyst acidity as very high or very low acidity could lead to low AL yields. According to the observations made in this study, the glucose conversion to AL is preferable using catalyst with moderate acidity.

4. CONCLUSION

The highest AL yields (ML: 14.67 wt%, EL: 15.04 wt%) obtained from glucose conversions were using Brønsted-Lewis AC-S-Cu under conditions of 180 ˚C, 4 h, 0.6 g of glucose loading, 40 mL of ethanol and 0.3 g of AC-S-Cu. The Brønsted-Lewis dual acidity with significant Brønsted acid value of AC-S-Cu as detected in pyridine FTIR analysis, had greatly contributed to its high catalytic activity. The larger surface area and porosity are also a major factor in providing high AL yield. Thus, it can be deduced that AC-S-Cu is a potential catalyst that had exhibited its prominence in the direct alcoholysis of glucose to AL.

ACKNOWLEDGEMENTS

This work was sponsored by Universiti Teknologi Malaysia Fundamental Research (UTM FR) grant [Q.J130000.3846.22H57] and partly supported by Ministry of Higher Education Malaysia (MOHE) under the Fundamental Research Grant Scheme [FRGS/1/2020/TK0/UTM/02/1].

REFERENCES

[1] S. Wang, K. Komvopoulos, Sci Rep (2021) 3914.
[2] S.G. Krishnan, F.L. Pua, K. Palanisamy, S.N.S. Jaafar, K. Subramaniam, (2018) 870.
[3] Z Mohammadbagheri, A.N. Chermahini, (2020) 2229.
[4] Q. Guan, T. Lei, Z. Wang, H. Xu, L, Lin, G. Chen, X. Li, Z. Li, (2018) 150.
[5] C. Tempelman, U. Jacobs, J. Herselman, R.V. Driel, F. Schraa, J. Versijde, T.V. Waversveld, Y. Yagci, M. Barg, F. Smits, F. Kuijpers, K. Lamers, T. Remijn, V. Degirmenci, (2023) 106661.
[6] S.A. Sadeek, E.A. Mohammed, M. Shaban, M.T.H.A. Kana, N.A. Negm, (2020) 112749.
[7] M.M. Zainol, M. Asmadi, P. Iskandar, W.A.N.W. Ahmad, N.A.S. Amin, T.T. Hoe, (2021) 124686.
[8] M. Wang, L. Peng, X. Gao, L. He, J. Zhang, (2020) 1383.
[9] N. Ya'aini, G.K.A Pillay, A. Ripin, 7th CONCEPT, 27-28 November 2018, Johor, Malaysia, 2019, p. 90.
[10] T.M. Masikhwa, J.K. Dangbegnon, A. Bello, M.J. Madito, D. Momodu, N. Manyala, (2016) 60.
[11] C. Fan, V. Nguyen, Y. Zeng, P. Phadungbut, T. Horikawa, D. Do, D. Nicholson, (2015) 79.
[12] W. Gong, C. Chen, Y. Zhang, H. Zhou, H. Wang, H. Zhang, Y. Zhang, G. Wang, H. Zhao, (2017) 2172.
[13] S.Y. Lee, S.J. Park, (2012) 307.
[14] J. Heda, P. Niphadkar, V. Bokade, (2019) 2319.
[15] C. Chang, L. Deng, G. Xu, (2018) 197.
[16] A.H. Hassan, M.M. Zainol, K.R. Zainuddin, H.A. Rosmadi, M. Asmadi, N.A. Rahman, N.A.S. Amin, (2022) 264.
[17] F. Yang, J. Tang, (2019) 1403.
[18] G. Wang, Z. Zhang, L. Song, (2014) 1436.